Please provide feedback

Please support the ScholarWorks@UMBC repository by emailing scholarworks-group@umbc.edu and telling us what having access to this work means to you and why it's important to you. Thank you.

Enormous disc of cool gas surrounding the nearby powerful radio galaxy NGC 612 (PKS 0131−36)

B. H. C. Emonts,[1]* R. Morganti,[2,3] T. A. Oosterloo,[2,3] J. Holt,[4,5] C. N. Tadhunter,[4] J. M. van der Hulst,[3] R. Ojha[6] and E. M. Sadler[7]

[1]*Department of Astronomy, Columbia University, Mail Code 5246, 550 West 120th Street, New York, NY 10027, USA*
[2]*Netherlands Foundation for Research in Astronomy, Postbus 2, 7990 AA Dwingeloo, the Netherlands*
[3]*Kapteyn Astronomical Institute, University of Groningen, P.O. Box 800, 9700 AV Groningen, the Netherlands*
[4]*Department of Physics and Astronomy, University of Sheffield, Sheffield S3 7RH*
[5]*Leiden Observatory, Leiden University, P.O. Box 9513, 2300 RA Leiden, the Netherlands*
[6]*United States Naval Observatory/NVI, 2212 40th Pl NW #2, Washington, DC 20007, USA*
[7]*School of Physics, University of Sydney, NSW 2006, Australia*

ABSTRACT

We present the detection of an enormous disc of cool neutral hydrogen (H I) gas surrounding the S0 galaxy NGC 612, which hosts one of the nearest powerful radio sources (PKS 0131−36). Using the Australia Telescope Compact Array, we detect $M_{H I} = 1.8 \times 10^9$ M$_\odot$ of H I emission-line gas that is distributed in a 140-kpc wide disc-like structure along the optical disc and dust lane of NGC 612. The bulk of the gas in the disc appears to be settled in regular rotation with a total velocity range of 850 km s^{-1}, although asymmetries in this disc indicate that perturbations are being exerted on part of the gas, possibly by a number of nearby companions. The H I disc in NGC 612 suggests that the total mass enclosed by the system is $M_{enc} \approx 2.9 \times 10^{12} \sin^{-2} i$ M$_\odot$, implying that this early-type galaxy contains a massive dark matter halo. We also discuss an earlier study by Holt et al. that revealed the presence of a prominent young stellar population at various locations throughout the disc of NGC 612, indicating that this is a rare example of an extended radio source that is hosted by a galaxy with a large-scale star-forming disc. In addition, we map a faint H I bridge along a distance of 400 kpc in between NGC 612 and the gas-rich ($M_{H I} = 8.9 \times 10^9$ M$_\odot$) barred galaxy NGC 619, indicating that likely an interaction between both systems occurred. From the unusual amounts of H I gas and young stars in this early-type galaxy, in combination with the detection of a faint optical shell and the system's high infrared luminosity, we argue that either ongoing or past galaxy interactions or a major merger event are a likely mechanism for the triggering of the radio source in NGC 612. This paper is part of an ongoing study to map the large-scale neutral hydrogen properties of nearby radio galaxies and it presents the first example of large-scale H I detected around a powerful Fanaroff–Riley type II (FR-II) radio galaxy. The H I properties of the FR-II radio galaxy NGC 612 are very similar to those found for low-power compact radio sources, but different from those of extended Fanaroff–Riley type I (FR-I) sources.

Key words: ISM: kinematics and dynamics – galaxies: active – galaxies: evolution – galaxies: individual: NGC 612 – galaxies: interactions.

1 INTRODUCTION

Early-type galaxies are often believed to be gas-poor systems. However, recent studies show that the majority of nearby field early-type galaxies contain modest amounts of neutral hydrogen (H I) gas (Morganti et al. 2006), while at least 6–15 per cent of all nearby early-type galaxies even contain H I masses similar to that of the Milky Way,[1] often distributed in large-scale rotating discs and rings (Sadler, Oosterloo & Morganti 2002; Oosterloo et al. 2007). Early-type galaxies in clusters appear to be much more devoid of H I gas,

---

*E-mail: emonts@astro.columbia.edu

[1] $M_{H I, MW} = 5 \times 10^9$ M$_\odot$ (Henderson, Jackson & Kerr 1982).

as suggested by a recent H I survey of the Virgo cluster by di Serego Alighieri et al. (2007). Nevertheless, these recent results show that the gaseous component can be an important factor to consider in the hierarchical picture of galaxy formation.

Although *N*-body and hydrodynamic simulations investigate in detail the stellar component in the formation of early-type galaxies (e.g. De Lucia et al. 2006), the fate of the gas is much less clear. This is on the one hand related to the complicated feedback processes (such as star formation and outflow phenomena) that are effective on the gas, while on the other hand the processes of gas accretion are not yet well understood. The last factor being subject to a large range of possible accretion mechanisms, from the merging of two equal mass galaxies (e.g. Barnes 2002) or a more gradual infall of small gas-rich companions (e.g. van der Hulst & Sancisi 2005) to perhaps slow accretion through the cooling of primordial hot circumgalactic gas (e.g. Kereš et al. 2005).

Radio galaxies form an interesting subset in understanding the gaseous properties of early-type galaxies, because the triggering mechanism of radio sources is related to gas-dynamical processes that can remove enough angular momentum from the gas for it to be deposited on to a supermassive black hole in the centre of the galaxy. Various possible triggering mechanisms have been suggested, often for particular types of radio sources. These mechanisms range from cooling flows (e.g. Fabian 1994) to galaxy interactions, dry mergers (Colina & de Juan 1995) and major gas-rich collisions and mergers between equal mass galaxies (e.g. Heckman et al. 1986; Baum, Heckman & van Breugel 1992). The last group is particularly interesting with respect to investigating the hierarchical model of galaxy evolution, because the typical end product of a major merger between two gas-rich disc galaxies is an early-type galaxy (e.g. Naab, Burkert & Hernquist 1999).

A significant fraction of the more powerful, edge-brightened Fanaroff–Riley type II (FR-II; Fanaroff & Riley 1974) radio galaxies show optical peculiarities reminiscent of a gas-rich galaxy collision or merger (such as tidal-tails, -bridges, -plumes etc.; Heckman et al. 1986; Smith & Heckman 1989; Baum et al. 1992). Detailed studies of extended emission-line regions around powerful radio galaxies reveal that mergers or interactions are often associated with their early-type host galaxies (e.g. Tadhunter, Fosbury & Quinn 1989; Koekemoer & Bicknell 1998; Inskip et al. 2007; Fu & Stockton 2008). In addition, a number of FR-II radio galaxies have been studied in great detail to show evidence for the presence of an intermediate-age stellar population, likely the result of a merger-induced starburst (e.g. Tadhunter et al. 2005; Fu & Stockton 2008). This indicates that powerful radio galaxies are ideal cases to investigate in detail these active phases of galaxy evolution. Furthermore, feedback from active galactic nuclei (AGN) is more and more recognized to be a crucial factor in regulating the gas distribution and, related, the star formation properties of early-type galaxies (e.g. Di Matteo, Springel & Hernquist 2005; Hopkins et al. 2005; Springel, Di Matteo & Hernquist 2005). In recent studies, we find that the feedback effects of powerful radio sources on the interstellar medium (ISM) result in some cases in significant outflows of mostly neutral hydrogen gas from the central region of the host galaxy (Morganti et al. 2003, 2005a,b; Emonts et al. 2005), indicating that the radio-loud phase may have a direct impact on the gaseous properties, and hence the evolution, of the galaxy.

The early-type galaxy NGC 612 is one of the nearest systems that contain a powerful radio source with FR-II properties. NGC 612 is therefore is an excellent candidate to investigate in detail the presence and possible distribution of gas and compare this to the origin of the system and triggering of the radio source. In this paper

we present results of a study of the neutral hydrogen (H I) 21-cm-line gas in NGC 612 and its environment. The combined spatial and kinematical information obtained with radio synthesis observations of the H I emission-line gas provides an efficient tool to study both the gas distribution and kinematics, as well as to trace, date and classify tidal signatures from galaxy interactions and mergers (tails, bridges, plumes, discs etc.). We compare our H I results with a stellar population analysis of NGC 612 done by Holt et al. (2007) and with the properties of the radio source. We also compare our findings with interesting results that we recently obtained on the H I content and distribution in lower power [compact and Fanaroff–Riley type I (FR-I)] radio galaxies (Emonts et al. 2007).

NGC 612

NGC 612 has been studied in detail by Véron-Cetty & Véron (2001) to be a typical S0 galaxy, which is located at $z = 0.0297$.[2] Goss et al. (1980) traced a regularly rotating emission-line disc out to a radius of 28 kpc along the major axis of the galaxy,[3] although the emission lines are weak (Westerlund & Smith 1966; Goss et al. 1980; Tadhunter et al. 1993). NGC 612 also has a prominent dust lane along the disc, almost perpendicular to the radio axis (e.g. Ekers et al. 1978; Véron-Cetty & Véron 2001). After initial reports by Tadhunter et al. (1993) about peculiar optical spectral features (strong and narrow absorption features and a weak 4000-Å break) and by Raimann et al. (2005) about the presence of young stellar populations in NGC 612, recently Holt et al. (2007) traced a young stellar population with age ∼0.04–0.1 Gyr throughout the stellar disc of the host galaxy.

The large-scale, two sided structure of the radio source PKS 0131−36 in host galaxy NGC 612 became apparent from radio observations by Ekers et al. (1978) and was studied at higher resolution by Morganti, Killeen & Tadhunter (1993). The eastern radio lobe has a clear FR-II (Fanaroff & Riley 1974) morphology, with a bright hotspot near its outer edge, while the western lobe is somewhat more diffuse. Gopal-Krishna & Wiita (2000) classified the radio source as a so-called HYMORS (HYbrid MOrphology Radio Source), with the eastern lobe of type FR-II and the western lobe of type FR-I. The total radio power is $P_{4.8\,\mathrm{GHz}} \sim 0.8 \times 10^{25}\,\mathrm{W\,Hz}^{-1}$ (Morganti et al. 1993),[4] which is at the border between the typical power of FR-I and FR-II sources (e.g. Owen & Laing 1989; Owen & White 1991; Ledlow, Owen & Eilek 2002). No bright optical AGN is apparent in NGC 612, given the weak optical emission lines (Tadhunter et al. 1993; Holt et al. 2007) and the low percentage of polarized light (Brindle et al. 1990) in the nuclear region.

2 OBSERVATIONS

The H I observations of NGC 612 were done with the Australia Telescope Compact Array (ATCA) for 2×12 h on 2003 June 25/26/27 using the 750C array configuration and for 2×12 h on 2005 October 10/11 using the EW214 array. Combining these two configurations gives a good *uv* coverage, with baselines ranging from 31 to 750 m for the inner five antennas of the array. The sixth ATCA antenna, located at a distance of about 5 km from the inner five antennas, was in operation only during the 750C configuration. We used this sixth antenna only for the very high spatial resolution absorption

---

[2] For $H_0 = 71\,\mathrm{km\,s}^{-1}\,\mathrm{Mpc}^{-1}$ (used throughout this paper); this puts NGC 612 at a distance of 125 Mpc and 1 arcsec = 0.6 kpc.
[3] Corrected for $H_0 = 71\,\mathrm{km\,s}^{-1}\,\mathrm{Mpc}^{-1}$.
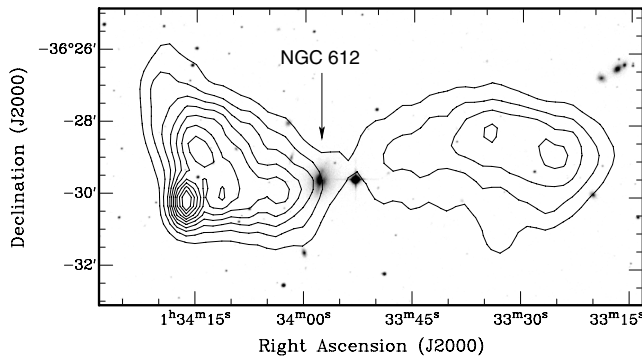[4] See footnote 3.

Figure 1. Radio continuum map (contours) – constructed from the 750C array data – overlaid on to an optical SDSS image of NGC 612 (grey-scale). Contour levels range from 41 to 468 in steps of 47 mJy beam^{-1}.

study described below. All observations were done with 16-MHz bandwidth, 512 channels and two polarizations.

For the data reduction and visualization we used the MIRIAD and KARMA software. After flagging and calibration, we separated the continuum from the line data in each individual data set by fitting either a first- or a second-order polynomial to the line-free channels. In order to trace the structure of the radio source in detail, the continuum data obtained with the 750C array (the configuration that provides the higher spatial resolution of the two) were used to create the uniform weighted continuum image shown in Fig. 1 [beam $= 62.4 \times 38.0$ arcsec^2; position angle (PA) $0.9°$]. The combined line data of all the four runs were used to construct a data cube with robust weighting $+1$ (see Briggs 1995), beam of 154.25×89.59 arcsec^2 (PA $-1.3°$), velocity resolution of 27.6 km s^{-1} (after binning two consecutive channels and subsequently Hanning smoothing the data) and noise level of 0.64 mJy beam^{-1}. From this data set a mask was created by smoothing the data spatially by a factor of 1.7, applying another Hanning smooth in velocity, and subsequently masking out all the signal below 3σ. This mask was used to extract a total intensity image of the data by adding the signal above 2.5σ in the regions that were not masked out (Fig. 2).

Finally, a continuum- and a line data set with the highest possible resolution were constructed from the 750C array data including the sixth ATCA antenna. As described in detail in Section 3.4, these data sets are not useful for accurate emission line or continuum studies (because of the gaps in *uv* coverage), but they are used for a detailed H I absorption analysis. Using uniform weighting, the beam size of these high-resolution data sets is 7.8×4.6 arcsec^2 (PA $-1.3°$), with a velocity resolution of 13.8 km s^{-1} for the line data.

2.1 VLT (Very Large Telescope) acquisition image

A short-exposure VLT acquisition image was taken with the FORS2 (Focal Reducer/low dispersion Spectrograph 2) instrument at ESO-VLT-U4 on 2003 September 25, using the R-Special filter. The integration time was 10 s and observations were done at an airmass of 1.1. The image consists of two simultaneous exposures at two separate chips, with a small overlap region to mosaic them. We did a bias subtraction and flat-fielding on each exposure before combing them. We then rotated the image to the north-up position shown in Fig. 7.

3 RESULTS

3.1 Radio continuum

Fig. 1 shows the continuum map of the radio source PKS 0131−36 in NGC 612. The map clearly shows the typical FR-II morphology of the eastern lobe (ending in a hotspot), while the western lobe appears to be more diffuse. The western lobe shows a slight bend, and also the eastern lobe looks somewhat distorted, suggesting that the radio source changed its direction over its lifetime. The total radio power that we derive for this source is $P_{1.4\,\mathrm{GHz}} \sim 1.5 \times 10^{25}$ W Hz^{-1}. Although we note that our spectral-line observations are not ideal for constructing a continuum image, these results are nevertheless in agreement with the 4.8 GHz observations by Morganti et al. (1993, see also section 1), when taking into account the spectral index of the radio source (see Wall & Peacock 1985).
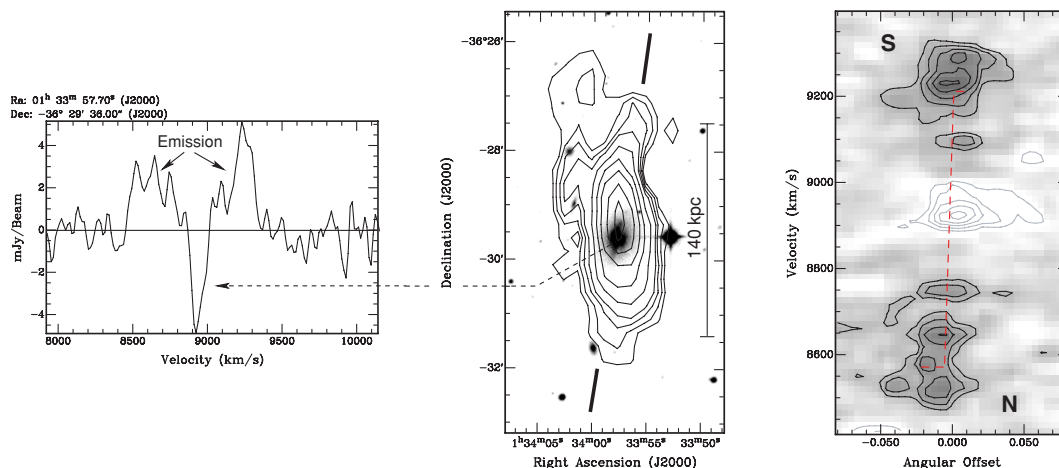

Figure 2. Middle: total intensity map of the H I gas in NGC 612 (contours) overlaid on to an optical SDSS image (grey-scale). Contour levels H I: 0.8, 1.1, 1.5, 1.9, 2.8, 4.0, 5.1, 6.5, 7.8 $\times 10^{19}$ cm^{-2}. Left: H I absorption profile against the central part of the radio galaxy. Right: position–velocity plot of the H I along the disc of the host galaxy (PA $171°$, as indicated by the broken line in the middle image). The dotted line presents the position–velocity curve derived from optical emission lines by Goss et al. (1980) measured along a slightly different PA ($168°$). Contour levels H I: -4.3, -3.6, -2.9, -2.2, -1.5 (grey); 1.5, 2.2, 2.9, 3.6, 4.3 (black) mJy beam^{-1}.
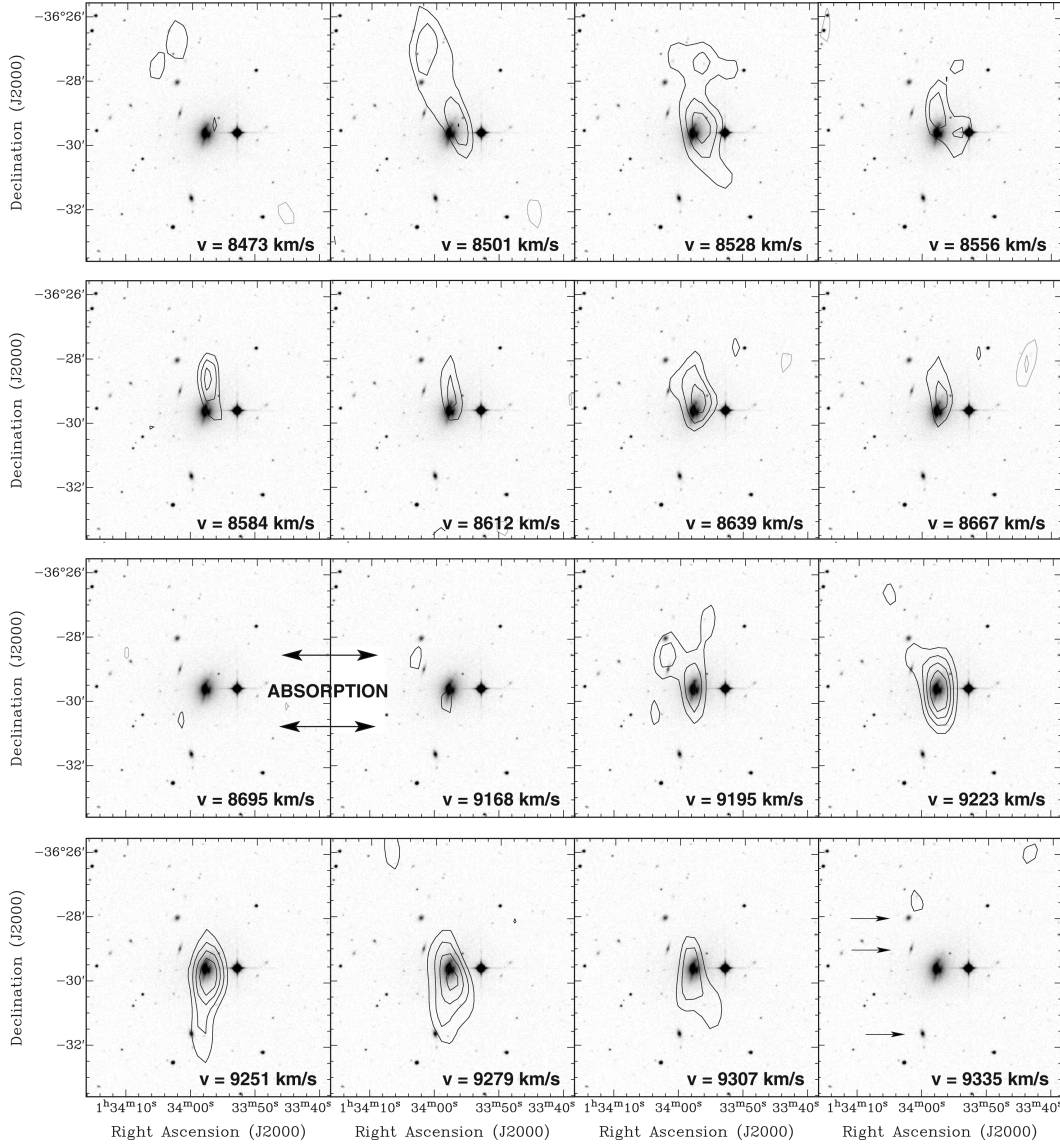
Figure 3. Channel maps of the H I emission in NGC 612. Contour levels are at the 3, 4, 5 and 6σ level, corresponding to -2.5, -1.9 (grey); 1.9, 2.5, 3.2, 3.8 (black) mJy beam^{-1}. The three possible small companions are indicated with an arrow in the last frame (see also Fig. 7).

3.2 H I emission

Fig. 2 (middle) shows a total intensity map of the H I gas detected in emission in NGC 612. The total mass of this H I gas is $1.8 \times 10^9 \, M_\odot$.[5] In the central region, H I is detected in absorption against the radio continuum (Fig. 2 – left), hence the total H I mass in NGC 612 is somewhat larger. Most of the H I gas in NGC 612 is located approximately along the direction of the optical disc and dust lane and has an average surface density at the location of the host galaxy of about 3.1 $M_\odot$ pc^{-2}. As illustrated in Figs 2 (right) and 3, the H I gas along the optical disc of NGC 612 appears to form a rotating structure (seen edge-on) with a total extent of about 140 kpc. This H I structure covers a velocity range of 850 km s^{-1}, centred on $v = 8900$ km s^{-1}. This is in good agreement with the central velocity of the H I absorption, which occurs at $v = 8925$ km s^{-1} (see also

Fig. 6) and which, we assume, indicates the systemic velocity of the system. The resolution of our observations is too low to determine the detailed morphology and kinematics of the H I gas and hence also whether or not the bulk of the H I is fully settled in regular rotation. Its kinematics nevertheless appear similar to those of the optical emission-line gas in this system, which has been observed by Goss et al. (1980) to follow regular rotation along the direction of the dust lane out to about 28 kpc from the centre, covering a velocity range of 680 km s^{-1} (centred on $v = 8900 \pm 50$ km s^{-1}).

Despite the apparent regular rotation, there is clearly some degree of asymmetry visible in the disc (the clearest asymmetries are visible in frames 2/3 and 11 of Fig. 3; i.e. at $v = 8501/8528$ and 9195 km s^{-1}). Because of the limited spatial resolution of our observations we cannot study these asymmetries in detail. Possibly, a warp in the disc of NGC 612 could be responsible for bending the disc at $v = 8501/8528$ km s^{-1}. Alternatively, the asymmetries may be tail-like features that stretch toward three small galaxies, whose redshifts are unknown. These galaxies are located 37 and 66 kpc north-east and 76 kpc south of NGC 612 spatially and are indicated

---

[5] All the H I mass estimates given in this paper have been corrected for the primary beam of the telescope.

with an arrow in the last plot of Fig 3. Fig. 7 shows these nearby galaxies in more detail. If these galaxies are true companions of NGC 612, the tail-like H I features could indicate that interactions are ongoing between them and the disc of NGC 612.

3.3 H I environment

Fig. 5 shows the total intensity H I map of the larger environment of NGC 612 at lower resolution (see below). The galaxy NGC 619 is located at a projected distance of 400 kpc east of NGC 612. The '8-shaped' optical appearance of NGC 619 is typical for galaxies with a prominent bar (e.g. Athanassoula & Bureau 1999). NGC 619 contains $8.9 \times 10^9 \, M_\odot$ of H I. Most of this H I gas is located at the position of the host galaxy. A prominent tail of H I gas stretches 219 kpc toward the south-west. This H I tail has no identifiable counterpart in the optical Sloan Digital Sky Survey (SDSS) image shown in Fig. 5.

When inspecting the data cube in the *xz* [right ascension (RA)–velocity] plane, we find clear evidence for additional, but very faint, H I emission-line gas in the region between NGC 612 and 619. This gets clear from Fig. 4. Here we show consecutive maps, plotted in velocity against RA, with the integrated signal across 44.7 arcsec (or 26.8 kpc) in declination (Dec.; to clarify the faint emission, the full-resolution data were smoothed in the image domain by 10 per cent in the spatial directions). Given the large beam size of the observations, the consecutive plots in Fig. 4 are not entirely independent. Nev-

ertheless, there are a few interesting features that emerge in Fig. 4. The emission in regions 1 and 2 is directly related to NGC 612 and 619. The H I tail south-west of NGC 619 is clearly visible in the third and fourth frame (arrow). This tail connects to a faint stream of H I in the direction of NGC 612 (feature '3', as indicated in the eighth frame). The faint H I stream – most likely some sort of bridge between both systems – appears to end at the central region as well as the systemic velocity of NGC 612. Because this H I bridge is detected only at about the 3σ level and the feature is extended in *x* and *y*, but not much in *z*, this feature is not immediately apparent in the *xy* planes of the data cube or in a total intensity image of the full resolution data. In order to give an indication of the spatial distribution of the H I bridge, we smoothed our data spatially to a resolution of 218.1×178.4 arcsec^2 and we applied an additional Hanning smooth in velocity. Fig. 5 shows a total intensity map made from this smoothed data by summing all the signal above 3σ only in the velocity range of the emission features. The H I tail south-west of NGC 619 and the connecting faint stream or bridge of H I in the direction of NGC 612 (feature '3') are clearly visible in this image. We note, however, that additional observations are required to accurately map the H I bridge spatially.

3.4 H I absorption

H I is detected in absorption at the location of the host galaxy. Fig. 2 (left) shows the absorption profile from the data cube that we used
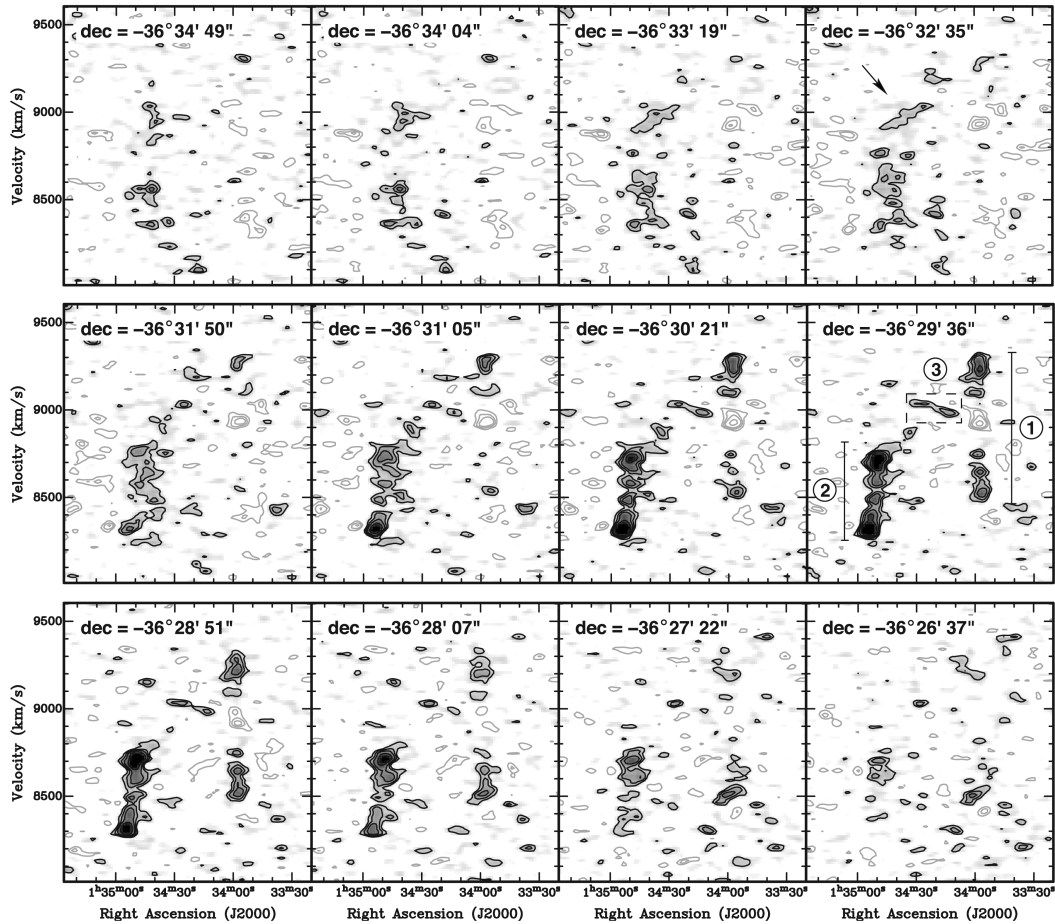

Figure 4. Consecutive maps (plotted in velocity versus RA) of the data cube. Every channel contains the integrated signal across 44.7 arcsec (or 26.8 kpc) in Dec. Contour levels are at the 2, 3, 4 and 6σ level (black for emission, grey for absorption). The features 1, 2 and 3, as well as the arrow, are discussed in the text and are also presented in the total intensity image of Fig. 5.
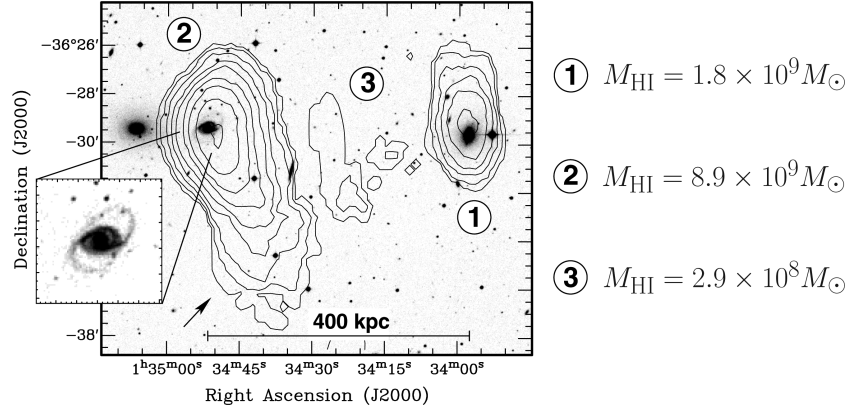
Figure 5. Total intensity map of H I emission from the low-resolution smoothed data cube (contours) overlaid on to an optical SDSS image (grey-scale). Contour levels: 0.2, 0.4, 0.7, 1.1, 1.7, 2.3, 3.4, 4.5, 5.7 $\times\,10^{19}$ cm^{-2}. The arrow indicates the prominent H I tail, which is the same feature marked by the arrow in Fig. 4.
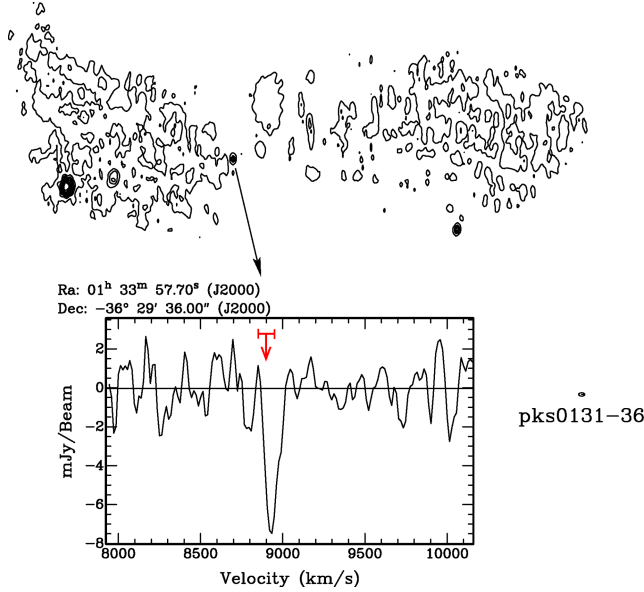

Figure 6. Top: high-resolution continuum image of PKS 0131−36 (NGC 612) including the sixth ATCA antenna. Contour levels: from 3.4 to 63 in steps of 8.5 mJy beam^{-1}. Bottom: H I absorption profile detected against the unresolved radio core. For comparison, the arrow indicates the systemic velocity derived from optical emission lines by Goss et al. (1980).

for the H I emission study (with robust weighting +1). In this data cube, the absorption profile is diluted by H I emission. In order to study the absorption in more detail, we made a high-resolution data cube using the 750C data plus the sixth ATCA antenna (see Section 2). The result is shown in Fig. 6. The high-resolution radio continuum map including the sixth antenna misses data from baselines between 750 m and about 4 km, which results in a large gap in *uv* coverage. Because there is no information about the structure of the radio source at the spatial scales that correspond to the gap in *uv* coverage, much of the extended continuum emission is resolved out in the resulting high-resolution continuum image. However, the long baselines of the sixth antenna allow us to trace the nucleus as an unresolved point source, which is not detected in the lower resolution continuum image in Fig. 1. By constructing also a uniform weighted data cube (in which the large-scale H I emission is

resolved out), we are able to recover the total flux of the H I absorption feature detected in the robust weighted data (as measured from the peak of the emission in Fig. 2) against the very core of the radio source (Fig. 6 – bottom). The radio continuum outside the core in Fig. 6 is too weak to detect absorption of H I gas with similar column densities.

The absorption has an optical depth of $\tau \sim 28$ per cent and full width at half-maximum (FWHM) ~ 100 km s^{-1}, which corresponds to a column density of $N_{\mathrm{H\,I}} \sim 5.1 \times 10^{21}$ cm^{-2} (for $T_{\mathrm{spin}} = 100$ K). This column density is significantly larger than that derived from the lower resolution emission-line data (Fig. 2). However, the H I absorption traces gas in our line-of-sight roughly through the midplane of the edge-on disc, whose scaleheight is much smaller than the large beam size of the emission-line study. Beam-smearing effects could therefore severely underestimate the true column densities of the H I disc in the emission-line analysis (locally, this effect could even be enhanced if the H I gas in the disc is clumpy). Alternatively, a substantial part of the absorbing gas may be located very close to the nucleus (e.g. in a nuclear disc or torus).

Against the eastern radio hotspot, no H I has been detected in absorption down to a 5σ level of $\tau \sim 0.6$ per cent (for the robust +1 data). This corresponds to an upper limit in H I column density of $N_{\mathrm{H\,I}} \lesssim 1 \times 10^{20}$ cm^{-2} (for FWHM = 100 km s^{-1} and $T_{\mathrm{spin}} = 100$ K) that lies in our line-of-sight to the radio hotspot.

3.5 Optical shells

Fig. 7 shows the VLT acquisition image (Section 2.1) of the environment of NGC 612. Although a high quality image of NGC 612 itself with a limited field-of-view has already been analysed by Véron-Cetty & Véron (2001), this acquisition image is the best available image for studying the optical structure of NGC 612 at the location of the outer disc and for identifying small galaxies surrounding NGC 612.

As mentioned in Section 3.2, part of the H I emission in the disc of NGC 612 seems to extend in the direction of three nearby small galaxies. These three galaxies are clearly visible in Fig. 7 – left (indicated with an arrow, as in Fig. 3). A redshift determination of these galaxies is necessary to verify whether these systems are true companions of NGC 612 or background objects. In addition, many other galaxies are visible in the VLT acquisition image.
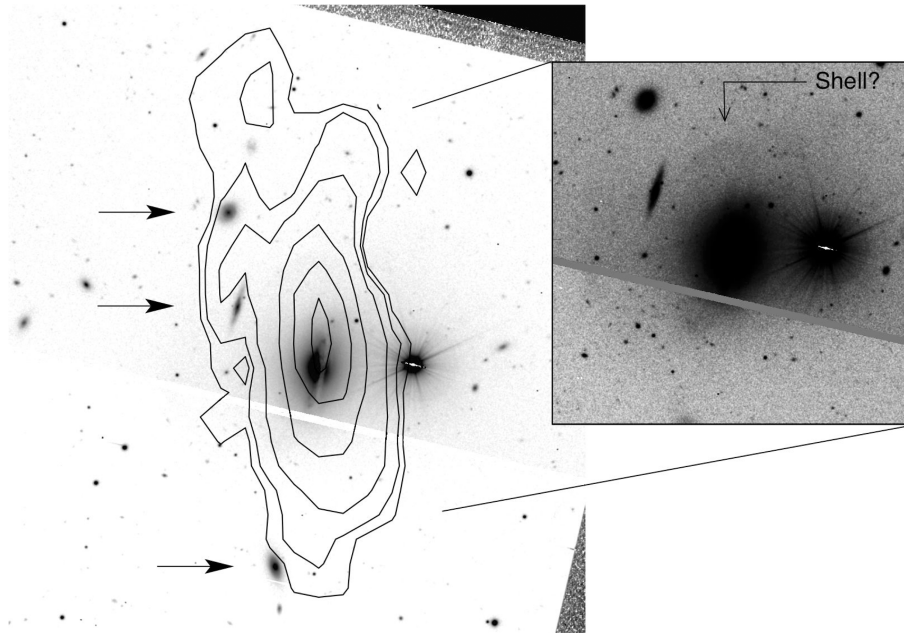
Figure 7. Left: contours of H I emission overlaid on to the optical VLT acquisition image (Section 2.1) of NGC 612 and its direct environment. Contour levels: 0.8, 1.1, 1.9, 4.0, 6.1, 7.8 $\times$ 10^{19} cm^{-2}. Right: high-contrast plot of the VLT acquisition image of NGC 612. The diagonal line across the image is the overlap region of the two chips (see Section 2.1).

Fig. 7 (right) shows NGC 612 in high contrast. A very faint shell-like structure is visible in this plot. The apparent optical shell is visible across the northern part of NGC 612, just west of one of the three small nearby galaxies toward which part of the H I structure appears to extend. A possible very faint optical extension may also be present in the southern part of NGC 612, although this needs to be verified. Since the integration time of our acquisition image is only 10 s, deep optical imaging should reveal these faint optical structures in much more detail.

4 DISCUSSION

We detect large-scale H I in the nearby radio galaxy NGC 612. The fact that NGC 612 harbours a powerful radio source with a clear hotspot in one of the jet/lobe structures makes it one of the few powerful FR-II radio galaxies – given their low volume density in the nearby Universe – for which accurate mapping of the H I emission-line gas can be done with the sensitivity of current-day radio telescopes. However, in the remainder of the discussion we would like the reader to keep in mind that, rather than being the nearby counterpart of powerful high z FR-II radio galaxies and quasars, the radio source properties of NGC 612 resemble more closely those found in the transition region between FR-I and FR-II sources (see Section 1).

4.1 Star-forming H I disc

NGC 612 contains a large-scale, edge-on H I disc, which appears to follow the optical disc and dust lane, but is observed out to a larger radius than the optical emission-line disc. The bulk of the H I gas in the disc appears to be settled in regular rotation, although asymmetries in the H I distribution – likely the result of either a warp or tidal interactions with small companion galaxies – indicate that perturbations are being exerted on part of the gas in the disc. Goss et al. (1980) estimate that the optical B-band luminosity of

NGC 612 is $L_B = 2.0 \times 10^{11}$ L$_\odot$, which means that $M_{\rm H I}/L_B = 0.009$ for this system (please note that this estimate does not take into account the H I gas detected in absorption against the central radio continuum, hence the true value of $M_{\rm H I}/L_B$ could be somewhat larger). From a literature study on a heterogeneous sample, Wardle & Knapp (1986) derive that about 24 per cent of nearby S0 galaxies have been detected in H I. The $M_{\rm H I}/L_B$ that we derive for NGC 612 is within the broad range, albeit at the low end, of the distribution for these H I detected S0 galaxies from the literature. The broad distribution of $M_{\rm H I}/L_B$ values in S0 galaxies has led Wardle & Knapp (1986) to conclude that much of the cold gas in S0s, like in ellipticals, has an origin completely external to the galaxy.

The average surface density of the H I disc in NGC 612 at the location of the optical host galaxy (3.1 M$_\odot$ pc^{-2}) is close to the critical gas surface density for star formation in galaxy discs (van der Hulst et al. 1993; Martin & Kennicutt 2001). As a result, star formation is likely to happen across the disc, or at least at discrete locations, where the H I surface density is locally higher than the average value derived from our H I observations. This is in agreement with the presence of a prominent young stellar population that has been traced throughout the stellar disc by Holt et al. (2007) out to a radius of at least 15 kpc.

4.1.1 Dark matter halo

Assuming the H I gas in the disc of NGC 612 follows regular rotation and the underlying dark matter halo has a spherical distribution, we can make an estimate of the total mass enclosed by the system:

$$M_{\rm enc} = \frac{R_{\rm out} v_{\rm out}^2}{\sin^2 i \; G}, \tag{1}$$

with $R_{\rm out}$ the outer radius of the rotating disc, $v_{\rm out}$ the observed velocity of the disc at this distance, i the inclination of the disc and $G = 6.673 \times 10^{-11}$ m^3 kg^{-1} s^{-2} the gravitational constant. Assuming $R_{\rm out} = 70$ kpc and $v_{\rm out} = 425$ km s^{-1} for NGC 612,

$M_{\mathrm{enc}} = 2.9 \times 10^{12} \sin^{-2} i\, \mathrm{M}_\odot$ (with i close to 90°). This is more than twice the value estimated by Goss et al. (1980) from the optical emission-line disc (which is much less extended than the H I disc and shows a slightly lower rotational velocity). Our estimate is most likely an upper limit, because a more flattened distribution of the underlying dark matter halo would decrease M_{enc}. Moreover, as we mentioned before, due to the limited resolution of our observations it is not exactly clear how settled the gas is in regular rotation, in particular in the outer parts of the disc. Nevertheless, given that NGC 612 has a luminosity of $L_B = 2.0 \times 10^{11}\,\mathrm{L}_\odot$ (Goss et al. 1980), we estimate that $M_{\mathrm{enc}}/L_B \leqslant 14.5$, which indicates that NGC 612 is likely embedded in a massive dark matter halo. Whether or not early-type galaxies *in general* contain significant amounts of dark matter is still under debate (see e.g. Romanowsky et al. 2003; Humphrey et al. 2006), but our derived value of M_{enc}/L_B for NGC 612 is in good agreement with M_{enc}/L_B for various early-type galaxies that also contain a large-scale rotating H I structure (see e.g. Bertola et al. 1993; Franx, van Gorkom & de Zeeuw 1994; Morganti et al. 1997; Weijmans et al. 2008, and other references therein).

4.1.2 Infrared properties

NGC 612 also has a relatively high infrared (IR) luminosity; from the *IRAS* flux measurements at 12–100 μm (Knapp et al. 1989) and following Sanders & Mirabel (1996) we estimate that the total IR luminosity of NGC 612 $L_{\mathrm{IR}}(8\text{–}1000\,\mu\mathrm{m}) = 4.3 \times 10^{11}\,\mathrm{L}_\odot$, which is in the regime of luminous infrared galaxies (LIRGs). In Fig. 8 we compare the relative 60 μm *IRAS* luminosity of NGC 612 with that of nearby early-type galaxies from a large sample studied by Knapp et al. (1989). We derive the 60 μm luminosity assuming $L_{60\,\mu\mathrm{m}} = 4\pi\nu S_\nu D^2/\mathrm{L}_\odot$, corresponding to $L_{60\,\mu\mathrm{m}} \approx 4 \times 10^{10}\,\mathrm{L}_\odot$ for NGC 612. Because our derived values for $L_{60\,\mu\mathrm{m}}$ and M_B do not take into account *K*-correction, reddening effects or true distance determination (which may affect in particular some of the nearest galaxies, whose redshift velocity may be dominated by gravitational motions due to surrounding galaxies), the values of $L_{60\,\mu\mathrm{m}}$ and M_B should be taken with caution. Nevertheless, the point that we want to make is that the 60 μm luminosity of NGC 612 is relatively high compared with that of genuine early-type galaxies (E and S0) up to distances comparable to that of NGC 612.

It is, however, known that radio-loud early-type galaxies on average contain a significantly larger 60 μm luminosity than their radio-quiet counterparts (Golombek, Miley & Neugebauer 1988; Knapp, Bies & van Gorkom 1990). In fact, when comparing NGC 612 with powerful radio galaxies in the nearby Universe (Golombek et al. 1988), a significant fraction of radio-luminous objects have a 60 μm luminosity comparable or larger than that of NGC 612 (and similar to that of spirals; de Jong et al. 1984). Although this fraction is somewhat smaller for radio galaxies with weak emission lines (like NGC 612), the emission-line region in NGC 612 is extended, which is an indication for the presence of an appreciable ISM that contributes to the IR luminosity (Golombek et al. 1988). It therefore seems that the IR luminosity of NGC 612 is strong compared to early-type galaxies in general, but not uncommon for powerful radio galaxies. Golombek et al. (1988) propose that galaxy–galaxy interactions can cause the strong IR emission and simultaneously trigger the activity in powerful radio galaxies.

Although a substantial part of the 60 μm emission in active galaxies often comes from a dust-enshrouded AGN, the lack of a powerful optical AGN in NGC 612 (see Section 1), combined with its relatively cool mid-IR colour (Knapp et al. 1989), implies that most of the 60 μm emission in this system is the result of dust heating by stars. Additional evidence for this comes from the fact that NGC 612 clearly lies above the correlation between
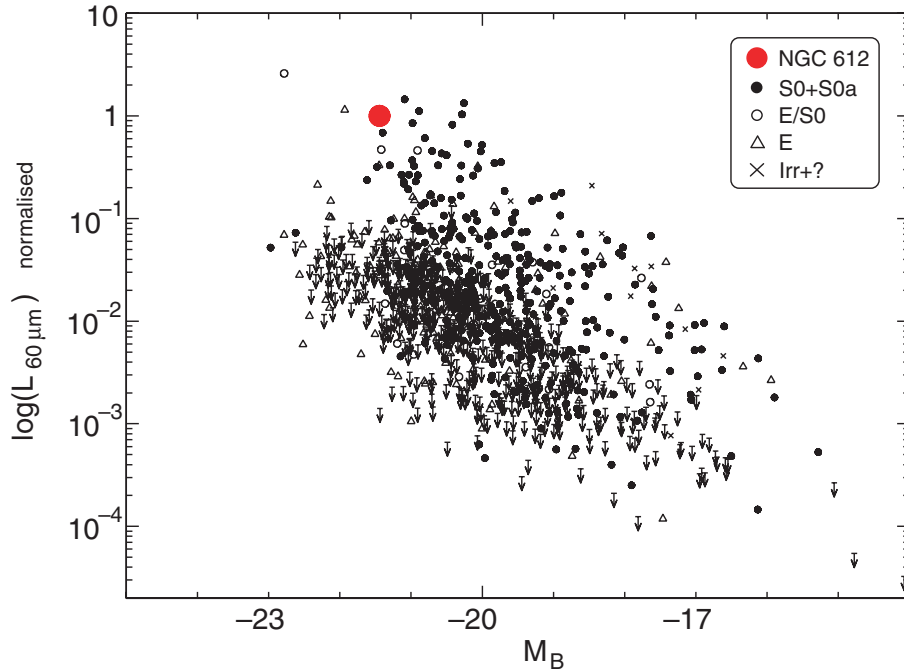

Figure 8. 60 μm *IRAS* luminosity of NGC 612 compared with that of a sample of nearby early-type galaxies (Knapp et al. 1989). The early-type galaxies are divided into S0 (and S0a) galaxies, transition objects (E/S0), ellipticals (E) and irregular/morphologically undefined galaxies (Irr+?), which are represented by the different symbols (as indicated in the plot). $L_{60\,\mu\mathrm{m}}$ (normalized to the value of NGC 612) and M_B are derived from $S_{60\,\mu\mathrm{m}}$, v and m_B as given by Knapp et al. (assuming the redshift velocity v gives a good indication of the distance to the galaxies). In case of a non-detection at 60 μm, a 3σ upper limit is plotted (arrows). Galaxies for which m_B or v was not given by Knapp et al., or which have a negative redshift velocity, were not taken into account.

the 70 μm IR luminosity and the [O III]λ5007 emission-line flux due to AGN heating in powerful radio galaxies presented by Tadhunter et al. (2007). It is interesting to note, however, that the IR colours of NGC 612 (with log[f_ν(60 μm)/f_ν(100 μm)] = −0.48 and log[f_ν(12 μm)/f_ν(25 μm)] = 0.20; Knapp et al. 1989) suggest that its IR flux does not originate entirely from actively star-forming regions associated with the young stellar population in NGC 612 (as is often the case for IR luminous starburst galaxies), but that an appreciable fraction likely comes from cirrus irradiated by the galaxy's total stellar population (see Helou 1986, note that the IR colours of NGC 612 are similar to e.g. those of M81). Detailed IR spectroscopy is required for a more quantitative analysis of the nature of the IR emission in NGC 612.

4.2 NGC 612, a special radio galaxy?

The presence of an extended H I and optical emission-line disc, a young stellar population at various locations in this disc, a massive dark matter halo and a high 60 μm IR luminosity suggest that NGC 612 – despite the fact that the host galaxy has a regular S0 optical morphology (Véron-Cetty & Véron 2001) – may be considered a star-forming disc galaxy (be it with a relatively large bulge), although it is not clear to how far out in the low surface brightness H I disc star formation occurs. If dust extinction is important in the relatively large column of cold gas along our line-of-sight to the edge-on H I disc, it is possible that a faint optical stellar counterpart in the outer parts of this disc may become visible only in deep optical imaging across a large enough field of view.

The occurrence of an extended radio source in a host galaxy with regular optical morphology and a galaxy-scale star-forming disc is a rare phenomenon. Véron-Cetty & Véron (2001) argue that almost all classical double radio sources in the nearby Universe (FR-Is and FR-IIs) are associated with elliptical galaxies, that the more discy S0 hosts are often misidentified ellipticals and that NGC 612 is therefore clearly an exception to the rule. This view is shared by Ledlow et al. (2001) and Keel et al. (2006), who studied in detail another exceptional case, namely the spiral host galaxy of the extended FR-I radio source 0313−192. Another spiral host galaxy with an H I disc and a radio source that reaches outside the optical body of the galaxy is B2 0722+30 (Capetti et al. 2000; Emonts et al. 2007), but its FR-I radio source is relatively weak and small compared with NGC 612 and 0313−192 and we will present a detailed analysis of this galaxy in a forthcoming paper.

Although the radio source in NGC 612 (with its clear FR-II morphology of the eastern lobe) is an order of magnitude more powerful than the edge-darkened FR-I radio source in the spiral galaxy 0313−192 (Ledlow et al. 2001; Keel et al. 2006), both radio galaxies share some striking similarities: NGC 612 and 0313−192 both contain a relatively luminous bulge compared with typical spiral galaxies, which generally reflects the presence of a relatively massive central black hole (e.g. Kormendy & Richstone 1995; Ferrarese & Merritt 2000; Gebhardt et al. 2000). Both galaxies also show indications that tidal encounters may have occurred, which could have resulted in enhanced fuelling of the central engine (see Section 4.3 for more details). In addition, in both NGC 612 and 0313−192 the radio jets are aligned almost perpendicular to the disc. A high-resolution continuum image of NGC 612 by Morganti et al. (1993) shows that the radio axis lies about 25° from the minor axis of the host galaxy in the plane of the sky. The radio source has a somewhat distorted structure outside the optical host galaxy, indicating that the source changed its direction over its lifetime and that the alignment of the radio axis could have been even closer to the minor axis at an earlier

stage. It is likely that this is the direction in which the radio jets encounter the least resistance from the ISM. A massive black hole, enhanced fuelling and/or minor resistance from the ISM might explain the presence of an extended radio source in both NGC 612 and 0313−192.

4.2.1 Hybrid radio source morphology

Gopal-Krishna & Wiita (2000) suggest that the radio source in NGC 612 has a rare hybrid morphology (see Section 1), in which case the western jet/lobe should be classified as FR-I like. The mere existence of hybrid radio sources has led Gopal-Krishna & Wiita (2000) to argue that the FR dichotomy is likely related to interactions between the radio jet and the ambient medium on kpc scales, rather than to intrinsic properties of the central engine. The presence of a large-scale disc of neutral hydrogen in the host galaxy of NGC 612 make this an interesting object for studying this possibility in more detail, but this is beyond the scope of this paper.

4.3 Galaxy interactions and radio source triggering

As mentioned in Section 1, a significant fraction of the host galaxies of powerful FR-II radio sources show signs of a past galaxy merger or interaction event in the form of a peculiar optical morphology or the characteristics of extended emission-line regions. In these studies, it is suggested that such an event may be related to the triggering of the powerful radio source. Also for NGC 612, our study indicates that galaxy collisions or interactions likely occurred, possibly related to the triggering of the radio source and the star formation in this early-type galaxy.

Perhaps the most convincing evidence for a past galactic encounter comes from the long H I tail/bridge structure between NGC 612 and 619, which suggests that an interaction or collision likely took place between these two galaxies. It is interesting to note that in the vicinity of NGC 612, the H I bridge is aligned in the same direction as the radio jets.

Figs 3 and 7 show that more recent tidal interactions could also be ongoing between NGC 612 and several small nearby galaxies, although (as mentioned in Section 3.2) independent redshift determinations of the small nearby galaxies are necessary to verify whether they are true companions or background objects. If confirmed, such tidal interactions are likely to induce perturbations in the disc of NGC 612, which could result in some of the observed asymmetries in the disc of NGC 612 and perhaps also the triggering of star formation and fuelling of the AGN.

Another possible scenario is that NGC 612 and its large-scale H I disc formed as a result of a major merger event (i.e. a merger between two roughly equal mass galaxies, of which at least one – and possibly both – were gas rich), which may also have triggered the powerful radio source. It is well established from numerical simulations that the formation of early-type galaxies can be explained by galaxy mergers with a wide range in parameters (e.g. Toomre & Toomre 1972; Bekki 1998; Naab et al. 1999). A major merger may also trigger a burst of star formation, which in the dusty environment of the merging galaxies enhances the system's IR luminosity (e.g. Mihos & Hernquist 1994). Simulations by di Matteo et al. (2007) show that different orbital parameters of the merging galaxies have a different effect on the tidal disruption of gaseous and stellar discs and that in particular direct encounters often create large gaseous tidal tails. Barnes (2002) shows that such expelled tidal material can – on timescales of one to several Gyr – be re-accreted on to the newly formed

host galaxy and settle into a large-scale gas disc. Observationally, two recent detailed case studies show that a large-scale, low-surface brightness H I disc can indeed form around an early-type host galaxy as a result of a major merger (Emonts et al. 2006; Serra et al. 2006).

For NGC 612, the early-type optical appearance of the host galaxy with a faint optical shell, the high IR luminosity and the presence of a massive, large-scale, low surface brightness H I disc indicate that a major merger event could have occurred also in this system, although additional observations are necessary to confirm this and to determine the fate of the gas during such a possible merger event. However, *if* a major merger formed NGC 612, it likely occurred several rotational periods (i.e. >Gyr) ago, after which the large-scale H I gas had time to settle in a regular rotating disc and the host galaxy to gain its primary early-type appearance. Such a time-scale is long compared to the typical spectral ages (10^6–10^7 yr) derived for extended FR-II radio sources (e.g. Alexander & Leahy 1987; Leahy, Muxlow & Stephens 1989; Liu, Pooley & Riley 1992; Parma et al. 2002), although Blundell & Rawlings (2000) and Parma et al. (2002) argue that the ages could be as much as 0.1–1 Gyr as a result of an erroneous approximation of the magnetic field in the traditional spectral ageing arguments, mixing of old and young electrons by back flow and continuous replenishment of energetic electrons. In addition, for radio sources in major merger systems, it is not uncommon that there is a significant time delay between the initial merger and the onset of the most recent period of radio-AGN activity (Tadhunter et al. 2005; Emonts et al. 2006). Therefore, the possibility that a merger event may have triggered the radio-AGN activity in NGC 612 – as is often suggested for other powerful FR-II radio galaxies – appears to be a viable scenario, but this needs to be verified with future observations.

An intriguing possibility is that the H I disc around NGC 612 may continuously accrete gas from either the large-scale H I bridge between NGC 612 and 619 or the small nearby companions. This could explain why the disc in NGC 612 is relatively large and massive, for example compared to the case of the nearby radio galaxy Centaurus A (Cen A), which – as we will describe in detail below – contains a much smaller disc as a likely result of an unequal mass merger (van Gorkom et al. 1990; Schiminovich et al. 1994).

4.4 Large-scale H I in radio galaxies

As mentioned in Section 1, recent studies reveal that large-scale, massive H I structures – similar to the one in NGC 612 – are detected in a significant fraction of nearby field early-type galaxies (Sadler et al. 2002; Morganti et al. 2006; Oosterloo et al. 2007). However, also around a number of nearby radio-loud early-type galaxies, large-scale H I structures are known to exist.

Cen A, the nearest radio galaxy in the Universe, contains an H I disc of $M_{\text{H I}} \approx 4.5 \times 10^8 \, \text{M}_\odot$ out to a radius of about 8 kpc from the centre (van Gorkom et al. 1990; Schiminovich et al. 1994, for a distance of 3.5 Mpc to Cen A). It also has faint shells with $1.5 \times 10^8 \, \text{M}_\odot$ of H I gas out to about 15 kpc from the nucleus, which might represent a partial ring that rotates in the same sense as the body of the host galaxy, possibly as a result of an unequal mass merger between a large elliptical and a smaller gas-rich companion (Schiminovich et al. 1994). The prominent galaxy-scale dust disc in Cen A, combined with two extended radio jets/lobes perpendicular to this dust disc, has often led to the comparison with NGC 612 (Westerlund & Smith 1966; Ekers et al. 1978). For Cen A, the total H I mass is low and the extent of the H I features is small compared with NGC 612 (with the bulk of the H I gas in Cen A located within the optical body of the host galaxy). Furthermore, the radio source in

Cen A, generally classified as FR-I, is almost an order of magnitude less powerful than the one in NGC 612.

Another southern radio galaxy that contains a large-scale H I disc ($M_{\text{H I}} = 1.5 \times 10^{10} \, \text{M}_\odot$ and diameter = 127 kpc for $H_0 = 71 \, \text{km s}^{-1} \, \text{Mpc}^{-1}$) is the early-type galaxy PKS 1718−649 (Veron-Cetty et al. 1995). The gas in the large-scale disc of this radio galaxy is perturbed and Veron-Cetty et al. propose that this is perhaps the result of a merger that involved at least one spiral galaxy. The radio source in PKS 1718−649 is compact and classified as a gigahertz-peaked spectrum (GPS) radio source (Tingay & de Kool 2003).

In order to investigate the large-scale H I properties of radio-loud early-type galaxies in a more systematic way, we recently concluded an H I study of a complete sample of nearby, non-cluster radio galaxies from the B2 catalogue (Emonts 2006; Emonts et al. 2007). The radio sources in these systems, all with radio power lower than NGC 612, have either a compact or a typical edge-darkened FR-I morphology and their host galaxies were a priori classified as genuine early-type systems. When comparing the H I properties of these B2 radio galaxies with those of NGC 612, there are some remarkable results; similar to the case of NGC 612, regular rotating large-scale H I discs and rings (with $M_{\text{H I}} \approx$ several $\times 10^8$–$10^{10} \, \text{M}_\odot$ and diameters of several tens to hundreds of kpc) have been detected around roughly 50 per cent of the radio galaxies that host a compact (<15 kpc) radio source, while none of the early-type host galaxies of the extended FR-I radio sources shows any H I in emission above a conservative detection limit of a few $\times 10^8 \, \text{M}_\odot$. This is visualized in Fig. 9, which is a plot from Emonts et al. (2007) that shows the total H I mass detected in emission around NGC 612 and the B2 radio galaxies plotted against the size of the radio source (for comparison, we also included Cen A and PKS 1718−649). The large-scale H I disc in NGC 612 morphologically resembles that of the H I-rich compact sources (although the total H I mass is still about an order of magnitude lower than that of the most massive of the H I discs found around the compact sources; Emonts et al. 2006, 2007). NGC 612 contains significantly larger amounts of extended H I than the FR-I sources in our B2 sample.

The very nearby FR-I radio galaxy Cen A (3.5 Mpc) appears to be an exceptional case regarding its H I content compared with the
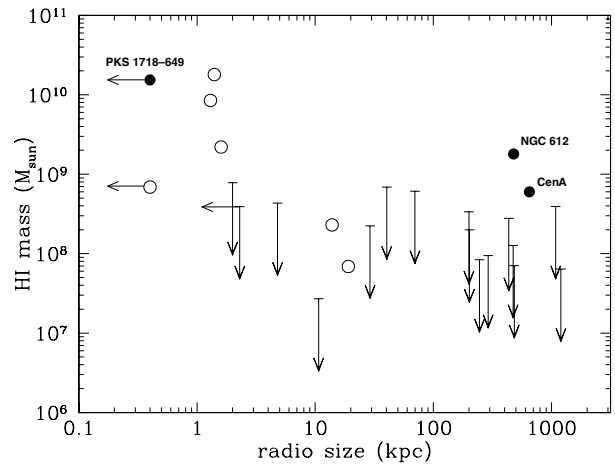

Figure 9. From Emonts et al. (2007): plot showing the total H I mass detected in emission plotted against the total linear extent of the radio source for our complete sample of B2 radio galaxies (open circles and upper limits) plus the three southern radio galaxies discussed in this paper (filled circles). In case of non-detection in the B2 sample, a conservative upper limit (3σ across 400 km s^{-1}) is given. See Emonts et al. (2007) for more details.

FR-I sources from our B2 sample. However, we note that the bulk of the detected H I emission in Cen A is – in contrast to most of our H I detections – located in a disc well inside the optical body of the host galaxy and part of this H I disc would have been observed in absorption against the central radio continuum instead of emission at the typical distance of most of our B2 sources (60–160 Mpc); see also Emonts et al. (2007). A detailed analysis will be postponed to a forthcoming paper.

We are currently conducting a study to map H I gas in a small but complete sample of the nearest FR-II radio galaxies in order to verify whether there is a fundamental difference in large-scale H I content between nearby FR-I and FR-II radio galaxies. Preliminary results appear to indicate that this may indeed be the case (Emonts et al. 2008), but final results on this will be presented in a future paper.

5 CONCLUSIONS

We presented results of a morphological and kinematical study of the neutral hydrogen gas in and around the nearby powerful radio galaxy NGC 612 (PKS 0131−36). We compared this with information about the stellar populations, optical morphology, IR characteristics and radio source properties of this radio-loud early-type galaxy. The most important conclusions that we discussed in this paper are the following.

(i) The S0 host galaxy NGC 612 contains a large-scale H I disc, with an H I mass of at least $1.8 \times 10^9 \, M_\odot$ and a diameter of about 140 kpc. The bulk of the H I gas appears to be in regular rotation, although asymmetries in the H I disc indicate that perturbations are being exerted on part of the gas, possibly by a number of nearby companions.

(ii) The total velocity range of the gas in the H I disc is $850 \, \mathrm{km \, s^{-1}}$, which indicates that NGC 612 contains a massive dark matter halo.

(iii) NGC 612 is a rare example of a galaxy with an extended radio source and a large-scale star-forming disc.

(iv) A long, faint H I bridge connects NGC 612 with the H I-rich barred galaxy NGC 619 about 400 kpc away, possibly as the result of a past interaction between both galaxies.

(v) We argue that – in agreement with what is generally observed for powerful FR-II radio galaxies – the triggering of the powerful radio source in NGC 612 could be related to ongoing or past galaxy interactions, or to a major merger event, which also may have formed the large-scale H I disc in NGC 612.

(vi) The large-scale H I properties of FR-II radio galaxy NGC 612 are similar to those of several nearby compact radio sources, but different from those of nearby FR-I sources.

Future studies are necessary to investigate in more detail the formation history of NGC 612 and compare this with the triggering and properties of its powerful radio source.

REFERENCES

Alexander P., Leahy J. P., 1987, MNRAS, 225, 1
Athanassoula E., Bureau M., 1999, ApJ, 522, 699
Barnes J. E., 2002, MNRAS, 333, 481
Baum S. A., Heckman T. M., van Breugel W., 1992, ApJ, 389, 208
Bekki K., 1998, ApJ, 502, L133
Bertola F., Pizzella A., Persic M., Salucci P., 1993, ApJ, 416, L45
Blundell K., Rawlings S., 2000, AJ, 119, 1122
Briggs D. S., 1995, PhD thesis, New Mexico Institute of Mining and Technology
Brindle C., Hough J. H., Bailey J. A., Axon D. J., Sparks W. B., 1990, MNRAS, 247, 327
Capetti A., de Ruiter H. R., Fanti R., Morganti R., Parma P., Ulrich M. H., 2000, A&A, 362, 871
Colina L., de Juan L., 1995, ApJ, 448, 548
de Jong T., Clegg P. E., Rowan-Robinson M., Soifer B. T., Habing H. J., Houck J. R., Aumann H. H., Raimond E., 1984, ApJ, 278, L67
De Lucia G., Springel V., White S. D. M., Croton D., Kauffmann G., 2006, MNRAS, 366, 499
Di Matteo T., Springel V., Hernquist L., 2005, Nat, 433, 604
di Matteo P., Combes F., Melchior A.-L., Semelin B., 2007, A&A, 468, 61
di Serego Alighieri S. et al., 2007, A&A, 474, 851
Ekers R. D., Goss W. M., Kotanyi C. G., Skellern D. J., 1978, A&A, 69, L21
Emonts B. H. C., 2006, PhD thesis, Univ. Groningen
Emonts B. H. C., Morganti R., Tadhunter C. N., Oosterloo T. A., Holt J., van der Hulst J. M., 2005, MNRAS, 362, 931
Emonts B. H. C., Morganti R., Tadhunter C. N., Holt J., Oosterloo T. A., van der Hulst J. M., Wills K. A., 2006, A&A, 454, 125
Emonts B. H. C., Morganti R., Oosterloo T. A., van der Hulst J. M., van Moorsel G., Tadhunter C. N., 2007, A&A, 464, L1
Emonts B., Morganti R., Oosterloo T., van Gorkom J., 2008, in Beswick R. J., Diamond P. J., Schilizzi R., eds, Proc. Sci., The Modern Radio Universe: From Planets to Dark Energy. In press (arXiv:0801.4769)
Fabian A. C., 1994, ARA&A, 32, 277
Fanaroff B. L., Riley J. M., 1974, MNRAS, 167, 31P
Ferrarese L., Merritt D., 2000, ApJ, 539, L9
Franx M., van Gorkom J. H., de Zeeuw T., 1994, ApJ, 436, 642
Fu H., Stockton A., 2008, ApJ, 677, 79
Gebhardt K. et al., 2000, ApJ, 539, L13
Golombek D., Miley G. K., Neugebauer G., 1988, AJ, 95, 26
Gopal-Krishna, Wiita P. J., 2000, A&A, 363, 507
Goss W. M., Danziger I. J., Fosbury R. A. E., Boksenberg A., 1980, MNRAS, 190, 23P
Heckman T. M., Smith E. P., Baum S. A., van Breugel W. J. M., Miley G. K., Illingworth G. D., Bothun G. D., Balick B., 1986, ApJ, 311, 526
Helou G., 1986, ApJ, 311, L33
Henderson A. P., Jackson P. D., Kerr F. J., 1982, ApJ, 263, 116
Holt J., Tadhunter C. N., González Delgado R. M., Inskip K. J., Rodriguez J., Emonts B. H. C., Morganti R., Wills K. A., 2007, MNRAS, 381, 611
Hopkins P. F., Hernquist L., Cox T. J., Di Matteo T., Martini P., Robertson B., Springel V., 2005, ApJ, 630, 705
Humphrey P. J., Buote D. A., Gastaldello F., Zappacosta L., Bullock J. S., Brighenti F., Mathews W. G., 2006, ApJ, 646, 899
Inskip K. J., Tadhunter C. N., Dicken D., Holt J., Villar-Martín M., Morganti R., 2007, MNRAS, 382, 95
Keel W. C., White R. E., III, Owen F. N., Ledlow M. J., 2006, AJ, 132, 2233
Kereš D., Katz N., Weinberg D. H., Davé R., 2005, MNRAS, 363, 2
Knapp G. R., Guhathakurta P., Kim D.-W., Jura M. A., 1989, ApJS, 70, 329
Knapp G. R., Bies W. E., van Gorkom J. H., 1990, AJ, 99, 476
Koekemoer A. M., Bicknell G. V., 1998, ApJ, 497, 662
Kormendy J., Richstone D., 1995, ARA&A, 33, 581
Leahy J. P., Muxlow T. W. B., Stephens P. W., 1989, MNRAS, 239, 401
Ledlow M. J., Owen F. N., Yun M. S., Hill J. M., 2001, ApJ, 552, 120
Ledlow M. J., Owen F. N., Eilek J. A., 2002, New Astron. Rev., 46, 343
Liu R., Pooley G., Riley J. M., 1992, MNRAS, 257, 545
Martin C. L., Kennicutt R. C., 2001, ApJ, 555, 301
Mihos J. C., Hernquist L., 1994, ApJ, 431, L9

Morganti R., Killeen N. E. B., Tadhunter C. N., 1993, MNRAS, 263, 1023

Morganti R., Sadler E. M., Oosterloo T., Pizzella A., Bertola F., 1997, AJ, 113, 937

Morganti R., Oosterloo T. A., Emonts B. H. C., van der Hulst J. M., Tadhunter C. N., 2003, ApJ, 593, L69

Morganti R., Oosterloo T. A., Tadhunter C. N., van Moorsel G., Emonts B., 2005a, A&A, 439, 521

Morganti R., Tadhunter C. N., Oosterloo T. A., 2005b, A&A, 444, L9

Morganti R. et al., 2006, MNRAS, 371, 157

Naab T., Burkert A., Hernquist L., 1999, ApJ, 523, L133

Oosterloo T. A., Morganti R., Sadler E. M., van der Hulst T., Serra P., 2007, A&A, 465, 787

Owen F. N., Laing R. A., 1989, MNRAS, 238, 357

Owen F. N., White R. A., 1991, MNRAS, 249, 164

Parma P., Murgia M., de Ruiter H. R., Fanti R., 2002, New Astron. Rev., 46, 313

Raimann D., Storchi-Bergmann T., Quintana H., Hunstead R., Wisotzki L., 2005, MNRAS, 364, 1239

Romanowsky A. J., Douglas N. G., Arnaboldi M., Kuijken K., Merrifield M. R., Napolitano N. R., Capaccioli M., Freeman K. C., 2003, Sci, 301, 1696

Sadler E. M., Oosterloo T., Morganti R., 2002, in Da Costa G. S., Jerjen H., eds, ASP Conf. Ser. Vol. 273, The Dynamics, Structure and History of Galaxies: A Workshop in Honour of Professor Ken Freeman. Astron. Soc. Pac., San Francisco, p. 215

Sanders D. B., Mirabel I. F., 1996, ARA&A, 34, 749

Schiminovich D., van Gorkom J. H., van der Hulst J. M., Kasow S., 1994, ApJ, 423, L101

Serra P., Trager S. C., van der Hulst J. M., Oosterloo T. A., Morganti R., 2006, A&A, 453, 493

Smith E. P., Heckman T. M., 1989, ApJ, 341, 658

Springel V., Di Matteo T., Hernquist L., 2005, MNRAS, 361, 776

Tadhunter C. N., Fosbury R. A. E., Quinn P. J., 1989, MNRAS, 240, 225

Tadhunter C. N., Morganti R., di Serego-Alighieri S., Fosbury R. A. E., Danziger I. J., 1993, MNRAS, 263, 999

Tadhunter C., Robinson T. G., González Delgado R. M., Wills K., Morganti R., 2005, MNRAS, 356, 480

Tadhunter C. et al., 2007, ApJ, 661, L13

Tingay S. J., de Kool M., 2003, AJ, 126, 723

Toomre A., Toomre J., 1972, ApJ, 178, 623

van der Hulst J. M., Sancisi R., 2005, in Braun R., ed., ASP Conf. Ser. Vol. 331, Extra-Planar Gas. Astron. Soc. Pac., San Francisco, p. 139

van der Hulst J. M., Skillman E. D., Smith T. R., Bothun G. D., McGaugh S. S., de Blok W. J. G., 1993, AJ, 106, 548

van Gorkom J. H., van der Hulst J. M., Haschick A. D., Tubbs A. D., 1990, AJ, 99, 1781

Véron-Cetty M. P., Véron P., 2001, A&A, 375, 791

Veron-Cetty M.-P., Woltjer L., Ekers R. D., Staveley-Smith L., 1995, A&A, 297, L79

Wall J. V., Peacock J. A., 1985, MNRAS, 216, 173

Wardle M., Knapp G. R., 1986, AJ, 91, 23

Weijmans A.-M., Krajnović D., van de Ven G., Oosterloo T. A., Morganti R., de Zeeuw P. T., 2008, MNRAS, 383, 1343

Westerlund B. E., Smith L. F., 1966, Aust. J. Phys., 19, 181

This paper has been typeset from a TEX/LATEX file prepared by the author.